International Journal of Civil Engineering and
Geo-Environmental

Journal homepage:http://ijceg.ump.edu.my
ISSN:21802742

NUMERICAL SIMULATION OF SECONDARY SEDIMENTATION TANKS USING THE VOF METHOD FOR MODELING THE FREE SURFACE

Behzad Lak[1], Bahar Firoozabadi[1], Hossein Afshin[1], Ahmadreza Farizan[1]

[1]School of Mechanical Engineering, Sharif University of Technology, P.O. Box 11155-9567, Tehran, Iran.

ARTICLEINFO

Keywords:
secondary sedimentation tank
numerical simulation
VOF method
buoyancy forces,
particle size

A B S T R A C T

Secondary sedimentation tanks are one of the most important parts of water treatment plants. In these tanks, settling of suspended particles occurs by means of gravity. In the present study, flow in a rectangular secondary sedimentation tank has been investigated numerically using the VOF method for modeling the free surface and also the RNG $k-\epsilon$ model. In the presented model, in addition to the analysis of the free surface, the effect of the particle-particle interaction and buoyancy forces is also considered. Numerical simulations have been done using the open source software OpenFOAM. In order to model the particles in the flow, the relevant code has been expanded. By comparing the concentration values in the presence of particles with those from the experimental results, the importance of particle size distribution and changes in the particle size relative to the mean particle diameter can be observed. Furthermore, the results indicate that the performance of sedimentation tank is closely related to the size of the particles.

1.0 Introduction

Generally, the water available from the underground and surface resources is not directly potable and several physical and chemical processes need to be done in water treatment plants to treat the water. One of the most important and expensive phases of the water purification process is to separate contaminated suspended particles from water by means of gravity in sedimentation tanks. The geometrical shape of sedimentation tanks can be either rectangular or circular. Moreover, based on the sedimentation type and the use of coagulants, settling tanks are divided into two main categories: primary and secondary sedimentation tanks. In primary tanks which are used at the first stages of sedimentation, the size of the particles is large and their concentration is low. On the other hand, in secondary sedimentation tanks, the concentration of particles is high and their size is small. Because deposition of small particles by means of gravity requires a lot of time, coagulants are used in secondary sedimentation tanks. Due to the high concentration of particles in these tanks, the effect of particles on the hydrodynamics of the secondary tanks cannot be ignored in numerical simulations.

In sedimentation tanks, some hydraulic phenomena such as hydraulic short circuit, density waterfall and circulation zone can be observed. Hydraulic short circuit is a condition in which part or all of the inlet flow is directly connected to the outlet. In this condition, the particles don't have enough time for sedimentation and as a result, the tank efficiency decreases. When the inlet concentration becomes very high, the inlet flow moves toward the bed immediately after entering the tank. This phenomenon is called density waterfall. Due to the occurrence of the density waterfall, a high-velocity flow (density current) is formed near the tank bed which can suspend the deposited particles and brings them out of the tank. In addition, this high-velocity flow causes the particles to move faster along the tank length.

Nowadays, due to the high cost of experimental investigations, much attention has been paid to the numerical simulation of sedimentation tanks. Imam and McCorquodale(1983) study was one of the most fundamental numerical investigations about the settling tanks. This two-dimensional study has been done using the constant eddy viscosity model and the finite difference method. Tamayol et al. (2008b)examined the hydraulic efficiency of primary sedimentation tanks using the particle tracking method (PTM) and the Eulerian-Lagrangian simulation procedure. They used the flow through curves (FTC) method for comparing the tank efficiency in different cases. Their results showed that the PTM method can only be used at low concentrations. Al-Sammarraee et al. (2009a)numerically simulated the rectangular primary sedimentation tank using the large-eddy simulation (LES) method and the Smagorinsky model. They performed three-dimensional simulations for various particle sizes and compared their results with the results of the $k-\epsilon$ model and found that the results of the LES model are in much better agreement with the experimental results. Stamou and Gkesouli(2015b) studied the effect of the wind on the performance of primary sedimentation tanks in presence of the baffles and without baffles. They used the SST $k-\omega$ model and simulated the wind by applying a constant velocity (0.5 m/s) at the free surface and in the flow direction. They concluded that the wind has a negative effect on the tank performance.

Larsen (1977)was one of the first researchers who simulated the sedimentation tanks and observed the density waterfall phenomenon in them. Goula et al. (2008a)investigated the performance of secondary tanks in the presence of baffle using a two-dimensional model and a modified form of the $k-\omega$ model. They applied the effect of the particles by considering the drag force acting upon the particles and also their density. Fan et al. (2007)three-dimensionally examined the circular secondary tanks using the two-fluid model and determined the optimal height and radial position of the baffle in order to reduce the volume fraction of the particles at the outlet. Tamayol et al. (2009b)studied the effect of the buoyancy forces to determine the optimal location of the baffle in secondary sedimentation tanks. They simulated the turbulence using the standard $k-\epsilon$ model. Their results indicated that at high Reynolds numbers, the flow field and the optimal location of the baffle are independent of the inlet densimetric Froude number. Asgharzadeh et al. (2012)investigated numerically and experimentally the effect of the particles on the flow structure in secondary settling tanks. In order to consider the effect of the air above the free surface, they applied a constant shear stress at the free surface. They compared the velocity and concentration profiles with the experimental results and concluded that increasing the inlet concentration of particles reduces the circulation zone at the beginning of the channel.

In most investigations related to the sedimentation tanks, the free surface has been considered as a rigid lid with the symmetry boundary condition. Furthermore, in few studies which have been done using the VOF method, the effect of the particles and the buoyancy forces has not been examined. However, in reality, the surface tension and the shear stress due to the air above the tank affect the flow field. In the present research, a new model is used which considers the effect of the particles and their interactions and also the effect of the free surface for secondary sedimentation tanks. Velocity and concentration profiles are compared with the experimental results and the effect of the particle diameter and particle size distribution on the tank efficiency is examined.

2.0Mathematical model and the governing equations

In writing the conservation equations, it should be noted that the concentration of particles is not high enough to change the characteristics of the particle-laden fluid, including the viscosity. In vector notation, the continuity and momentum equations of the unsteady turbulent flow can be written as follows:

$$\frac{\partial \rho}{\partial t} + \nabla \cdot \left(\rho \vec{V}\right) = 0 \quad (1)$$

$$\frac{\partial (\rho \vec{V})}{\partial t} + \nabla \cdot \left(\rho \vec{V} \vec{V}\right) = -\nabla P + \nabla \cdot \left((\mu + \mu_t)\nabla \vec{V}\right) + \rho \vec{g'} \quad (2)$$

In the above equations, $\vec{V}$ is the velocity vector, p is the static pressure, ρ is the fluid density and μ is the fluid viscosity. In addition, μ_t is the eddy viscosity which will be explained later. Furthermore, Boussinesq approximation is used to model the Reynolds stresses. Also, g' is the reduced gravity acceleration which is due to the buoyancy forces and is defined as follows:

$$g' = g\frac{\rho_{mix} - \rho_w}{\rho_w} \quad (3)$$

where g is the gravitational acceleration and its value is equal to 9.81. In addition, ρ_{mix} is the density of particle-water mixture which is calculated from the following equation:

$$\rho_{mix} = \rho_w + C\left(\rho_p - \rho_w\right) \quad (4)$$

In equation (4), C is the volumetric concentration of particles and ρ_p is the particle density which is assumed 2650 kg/m^3 in the present study.

In order to simulate the sedimentation, the concentration equation is solved. This equation is written as:

$$\frac{\partial C}{\partial t}+\frac{\partial (uC)}{\partial x}+\frac{\partial (vC)}{\partial y}=\frac{\partial}{\partial x}\left(\frac{v_t}{\sigma_C}\frac{\partial C}{\partial x}\right)+\frac{\partial}{\partial y}\left(\frac{v_t}{\sigma_C}\frac{\partial C}{\partial y}\right)+\frac{\partial (v_s C)}{\partial y} \quad (5)$$

In the above equation, C is the volumetric concentration, u and v are flow velocities in x and y directions, and v_s is the fall velocity of the particles. In addition, σ_C is the Schmidt number and its value is assumed to be 1.

There are several relationships for obtaining the fall velocity of particles. The most important one is the Stokes law which is written as follows:

$$v_{stokes}=g{D_p}^2\frac{(\rho_p-\rho_w)}{18\mu} \quad (6)$$

where D_p is the mean diameter of particles. To obtain the above relation, it is assumed that a single spherical particle falls with a constant velocity and a Reynolds number of less than one. Moreover, the Stokes law does not consider the particle-particle interactions. In the present research,the double exponential relationship (which includes the effect of particle-particle interaction) has been used:

$$v_s=v_{stokes}\left[e^{-k_1(C-C_{\min})}-e^{-k_2(C-C_{\min})}\right] \quad (7)$$

In the above relation, $C_{\min}=0.002C_{\text{in}}$ and k_1 and k_2 are equal to 0.00565 and 0.02 respectively (Mccorquodale(1993)). In addition, v_{stokes} is the Stokes settling velocity which is determined from equation (6).

In order to simulate the free surface in the present study, the VOF method has been used. In this method, a scalar function called volume fraction of fluid(α) is used to determine the free surface. To specify the boundary between air and water, the volume fraction equation is solved. This equation is written as follows:

$$\frac{\partial \alpha}{\partial t}+\nabla\cdot\left(\alpha\vec{V}\right)=0 \quad (8)$$

The value of α obtained from equation (8) has a negligible error. As a result, a lot of research has been done to improve equation (8). Weller (2002)added another term (artificial compression) to equation (8) and rewrote the equation as:

$$\frac{\partial \alpha}{\partial t}+\nabla\cdot\left(\alpha\vec{V}\right)+\nabla\cdot\left(\overrightarrow{V_r}\alpha\left(1-\alpha\right)\right)=0 \quad (9)$$

where $\overrightarrow{V_r}=\overrightarrow{V_1}-\overrightarrow{V_2}$ is the relative velocity between the two phases (air and water) and is called the compression velocity. Moreover, $\vec{V}$ is equal to $\alpha\overrightarrow{V_1}+\left(1-\alpha\right)\overrightarrow{V_2}$.

In this study, RNG$k-\epsilon$ model is used to simulate the turbulence. Tamayol et al.(2006)noted that this model shows more accurately the behavior of the flow in sedimentation tanks as compared to the standard $k-\epsilon$ model. The turbulent kinetic energy k and turbulent dissipation ϵ are determined from the following equations (Yakhot(1986)):

$$\frac{D(\rho k)}{Dt}=\frac{\partial}{\partial x_j}\left(\alpha_k\mu_{eff}\frac{\partial k}{\partial x_j}\right)+G_k+G_b-\rho\varepsilon-Y_m+\mathrm{S}_k \quad (10)$$

$$\frac{D(\rho\varepsilon)}{Dt}=\frac{\partial}{\partial x_j}\left(\alpha_k\mu_{eff}\frac{\partial \varepsilon}{\partial x_j}\right)+C_{1\varepsilon}\frac{\varepsilon}{k}(G_k+C_{3\varepsilon}G_b)-C_{2\varepsilon}\frac{\rho\varepsilon^2}{k}-R_\varepsilon+\mathrm{S}_\varepsilon \quad (11)$$

In equations (10) and (11), G_k is the turbulent kinetic energy production due to the velocity gradients, G_b is the turbulent kinetic energy production due to the buoyancy and Y_M indicates the effect of fluctuations on the dissipation rate (ϵ) due to the compressibility. In addition, $C_{1\epsilon}$, $C_{2\epsilon}$ and $C_{3\epsilon}$ are constants, α_k and α_ϵ are the inverse of turbulent Prandtl numbers for k and ϵ, and S_k and S_ϵ are the sources defined by the user. G_k is calculated from the following relation:

$$G_k=-\rho\overline{u'_i u'_i}\frac{\partial u_i}{\partial x_j} \quad (12)$$

The eddy viscosity is determined by solving the following equation:

$$d\left(\frac{\rho^2 k}{\sqrt{\varepsilon\mu}}\right)=1.72\frac{\hat{\upsilon}}{\sqrt{\hat{\upsilon}^3-1+C_\upsilon}}d\hat{\upsilon} \quad (13)$$

in which $C_\upsilon=100$ and $\hat{\upsilon}=\frac{\mu_{eff}}{\mu}$(Yakhot(1986)).

R_ϵ in equation (11) is the main difference between the RNG and standard model and is calculated as

$$R_\epsilon = \frac{C_\mu \rho \eta^3 (1 - \frac{\eta}{\eta_0})}{1 + \beta \eta^3} \frac{\varepsilon^3}{k} \quad (14)$$

where β=0.0012, $\eta_0 = 4.38$ and $\eta = sk/\varepsilon$(Yakhot(1986)). S is the mean strain rate which is defined as:

$$S = \sqrt{\frac{1}{2}(\frac{\partial u_i}{\partial x_j} + \frac{\partial u_i}{\partial x_j})(\frac{\partial u_i}{\partial x_j} + \frac{\partial u_i}{\partial x_j})} \quad (15)$$

Due to the presence of the above expression, the RNG model more accurately predicts the circulation regions in the sedimentation tanks (as compared to the standard model).

Other important parameters in k and ϵ equations are turbulent prandtl numbers (α_k, α_ϵ) which are determined from an analytical relation and at high Reynolds numbers, $\alpha_k = \alpha_\epsilon \approx 1.393$. The values of other constants in the RNG model are $C_{1\epsilon} = 1.42$ and$C_{2\epsilon} = 1.68$(Yakhot(1986)).

3.0 Simulation method and Boundary conditions

The dimensions of the tank are shown in figure 1. Some experimental studiessuch asAsgharzadeh et al. (2011) carried out their experiments in this tank. Hence, the results obtained from the simulations are compared and validated with the results of Asgharzade et al.(2011)study. In order to apply the VOF method and determine the air-water interphase, the air above the tank should be considered in simulations. Therefore, air up to the height of 100 cm is also simulated.

The values of all variables are given at the entrance. The particle-laden flow is assumed to enter the channel with constant velocity of 2.69 cm/s in the horizontal direction. The inlet Reynolds number is 2959, based onthe inlet velocity and inlet height. follows:

Furthermore, the inlet concentration is assumed to be 1000 mg/lit.

According to thekleine and reddy(2005)study, $K_{in} = CU_{in}^2$ and $\varepsilon_{in} = C_\mu^{0.75} \frac{K_{in}^{1.5}}{l_m}$ are used to obtain the inlet turbulent kinetic energy and inlet dissipation rate. In these equations, C=0.2,C_μ=0.00845 and $l_m = 0.5HC_\mu$, where H is the channel height. It should be noted that$l_m$is called mixing length.

The outlet pressure is constant and equal to zero, and fully developed condition is considered for other quantities. The zero concentration gradient is applied on the walls, and standard wall function is employed for turbulence modelling.

The code has been developed by means of an open source CFD (OpenFOAM) software.This code uses the object-oriented programming language. Sinceby default, there was no solution in the software for the problem, some changes have been made in the interFoam option in order to add the concentration equation and buoyancy forces. In addition,finite volume method with collocated grid and PIMPLE algorithm has been used. Furthermore, to discretize the divergence and Laplacian terms, van Leer and 2nd order of upwind have been used. Moreover, central difference method has been used for the gradient terms.

4.0 Results

4.1 Grid independency

Three grid with 107500,129000 and 155000 meshes were investigated. In regions near the walls and also near the free surface, the grids are finer. Non-dimensional velocity and concentration profiles at x/L=0.75 are shown in figures 2 and 3 respectively. It can be seen that there is only a negligible difference between the results of the grids with 129000 and 155000 meshes. However, the difference between the 129000 and 107500 meshes is obvious. Therefore, grid with 129000 meshes is used for the comparison of the simulation results.

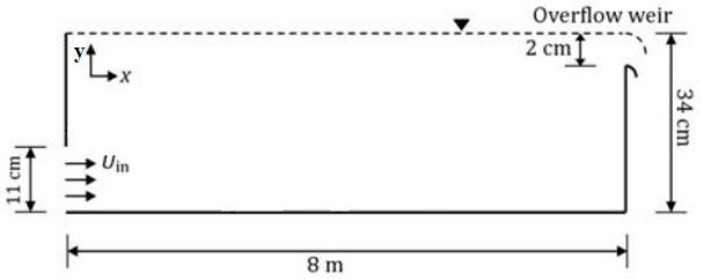

Figure 1: Tank dimensions

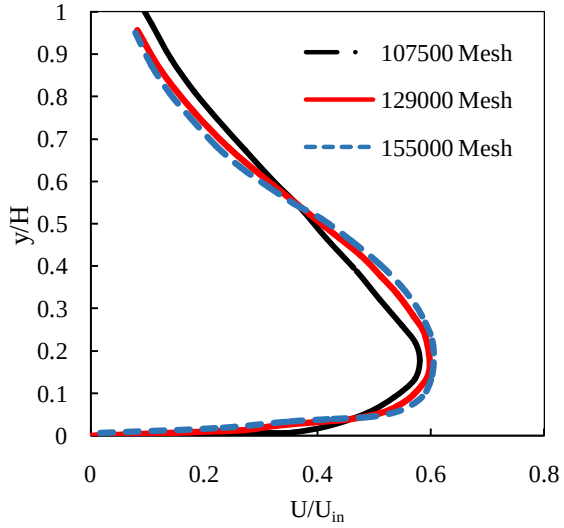

Figure 2: Velocity profiles for the investigationof grid independency at x/L=0.75

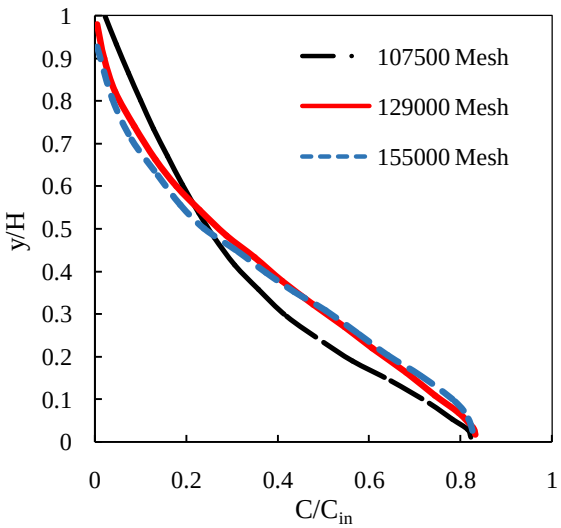

Figure 3: Concentration profiles for the investigation of grid independency at x/L=0.75

4.2 Analyzing the results

In this subsection, velocity and concentration profiles at different sections are examined and compared with the experimental results of Asgharzadeh et al.(2011).Considering that the mentioned particle size in the experimental study (12 µm) is the mean particle size for inlet particles, particles with larger diameters are also observed in the tank. Therefore, three separate simulations for particles with diameter of 8, 12 and 16 µm have been done. Concentration profiles along with the experimental results at x/L = 0.55, 0.625 and 0.75 are shown in figures 4 to 6 respectively. It should be noted that the investigated particle is kaolin with the density of 2650 kg/m^3.

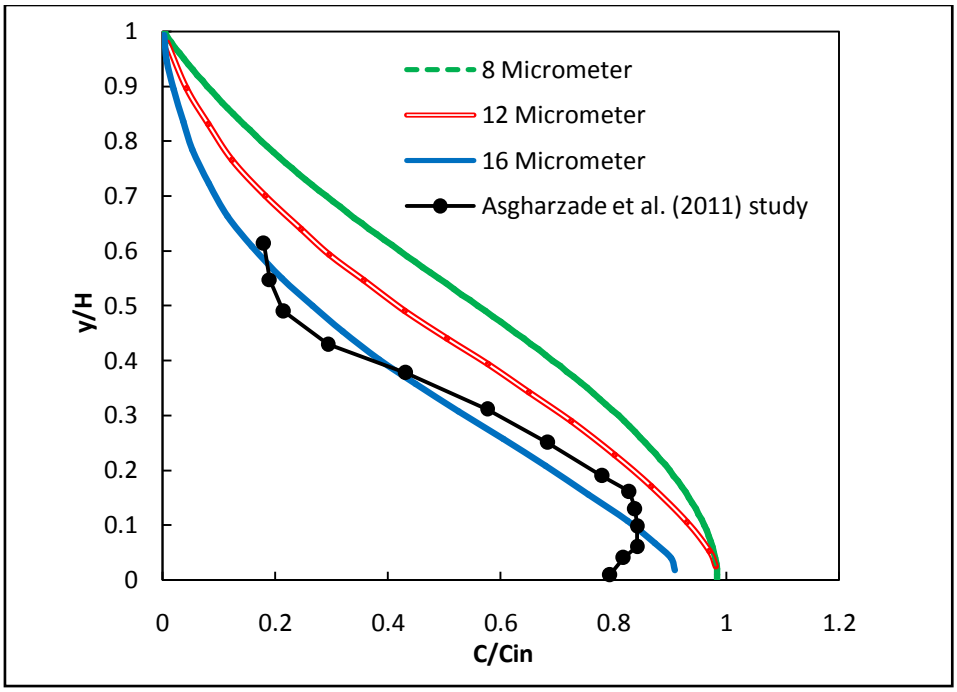

Figure 4: Concentration profiles at x/L=0.55 for various particle sizes

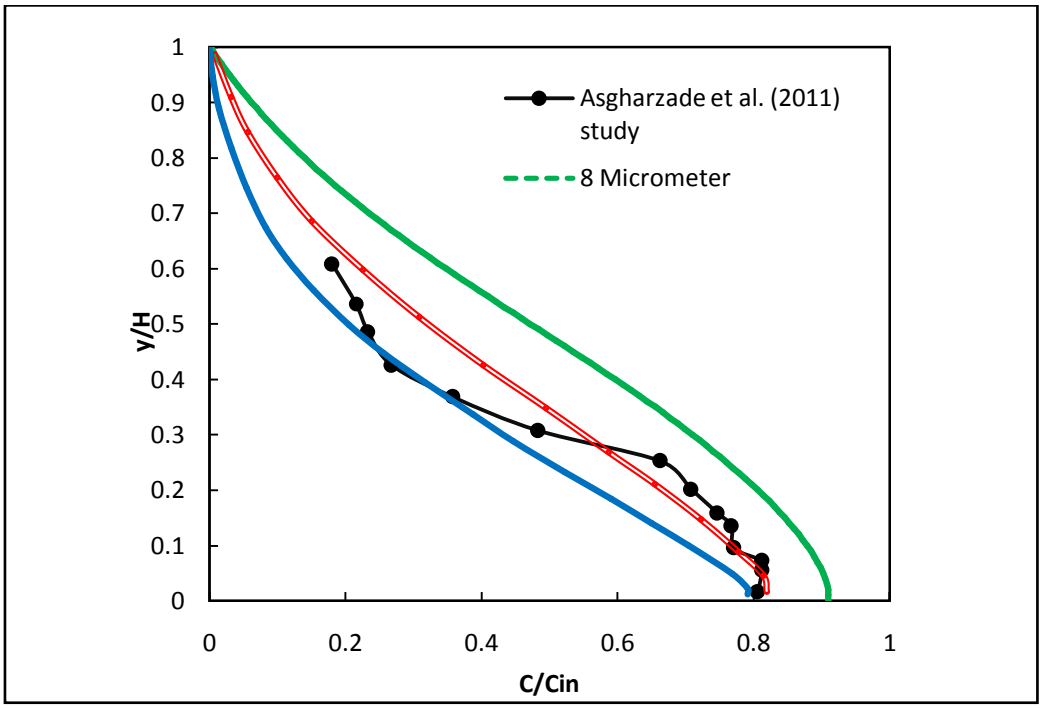

Figure 5: Concentration profiles at x/L=0.625 for various particle sizes

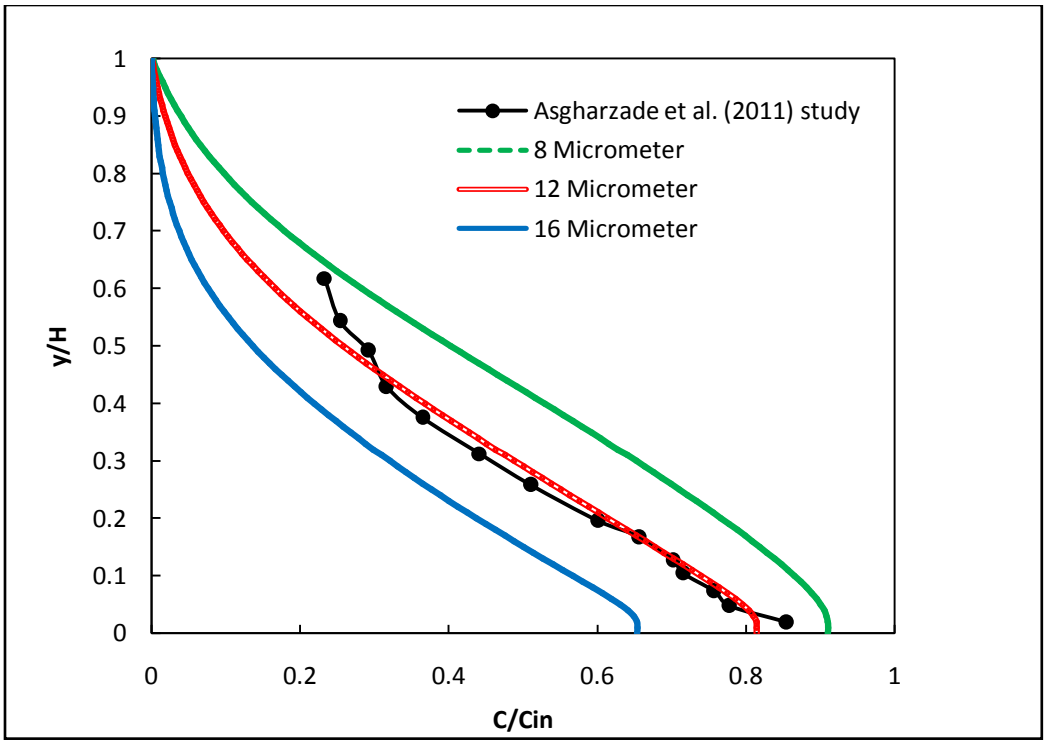

Figure 6: Concentration profiles at x/L=0.75 for various particle sizes

From these figures, it can be concluded that at x/L=0.55, the 16 µm concentration profileis nearly coincide with the experimental results. However, at sections farther from the inlet, the conformity of 12 µm particle results with theexperimental results becomes higher. For instance, at x/L=0.75, the concentration profile for 12 µm particles completely coincides with the experimental profile, while the difference between the results of 16µm particles and experimental results is relatively great. Moreover, at high distances from the bed (y/H>0.5) at x/L=0.75, the experimental concentration profile gets closer to the 8 µm concentration profile. This indicates that smaller particles exist at higher heights. Furthermore, it can be predicted that at locations near the outlet, the experimental profile gets much closer to the 8 µm concentration profile (however, the experimental data are not available at those locations). Therefore, the particle size distribution has a considerable effect on the concentration profile.

Velocity profiles at x/L=0.55, 0.625 and 0.75 are indicated in figures 7 to 9 respectively. It should be noted that the velocity profiles for the investigated particle sizes nearly coincide. Consequently, only one of the profiles has been compared with the experimental results. By comparing the velocity profiles with the experimental results, it can be seen that they are in good agreement with each other. At sections x/L=0.625 and 0.75, the maximum velocity is smaller than the maximum velocity of the experimental profile. This can be due to the fact that the numerical model is two-dimensional and therefore, three-dimensional effects were not considered in the simulations. Furthermore, it can be observed that the slope of the profiles is not zero at the free surface. As a result, the shear stress due to the presence of air at the top of the tank affects the velocity profiles. In addition, it can be seen that the maximum flow velocity slightly decreases along the channel length, because the concentration of particles and therefore the driving force of the current decreases along the channel.

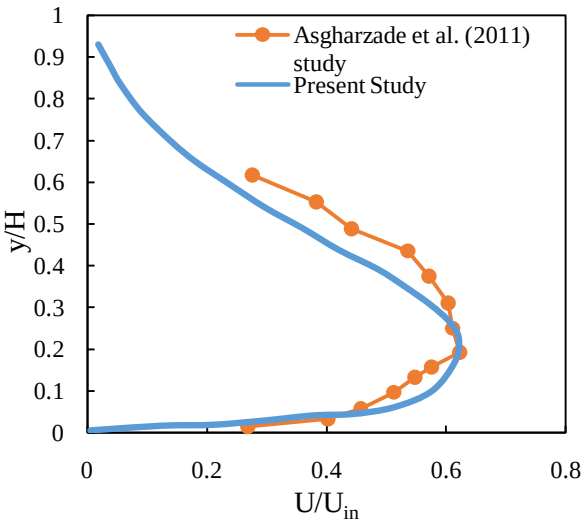

Figure 7: Comparison of velocity profiles with the experimental results at x/L=0.55

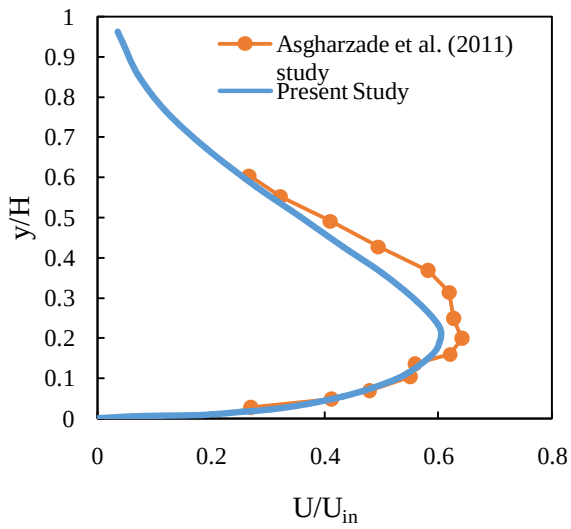

Figure 8: Comparison of velocity profiles with the experimental results at x/L=0.625

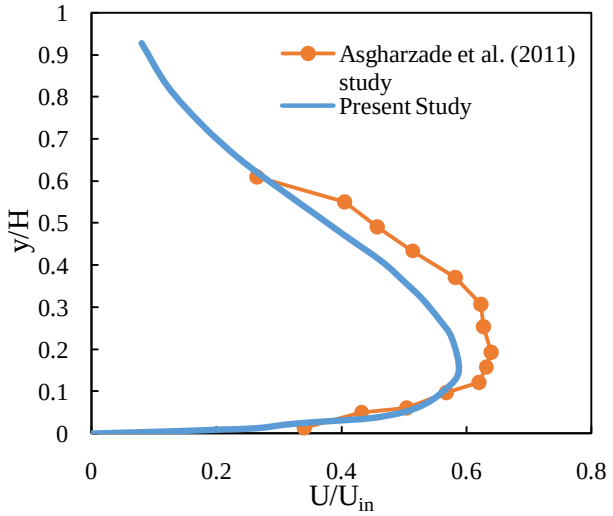

Figure 9: Comparison of velocity profiles with the experimental results at x/L=0.75

Figure10 illustrates changes in the mean concentration along the tank length for the three investigated diameters. The mean concentration is defined as follows:

$$\bar{C} = \frac{\int_0^H C\, dz}{H} \qquad (16)$$

in which H is the total height of the channel and is equal to 34 cm.

From this figure, it can be seen that the mean concentration decreases along the channel. Moreover, from x/L=0.2 to x/L=0.8, the slopes of the three curves are more than those near the inlet and outlet regions. This indicates that most sedimentation occurs between 0.2 and 0.8 of channel length. Furthermore, the most important result of this figure is the remarkable effect of particle size on the mean concentration. In all sections, a 4 µm increase in the particle size results in a 5 to 10 percent decrease in the mean concentration.

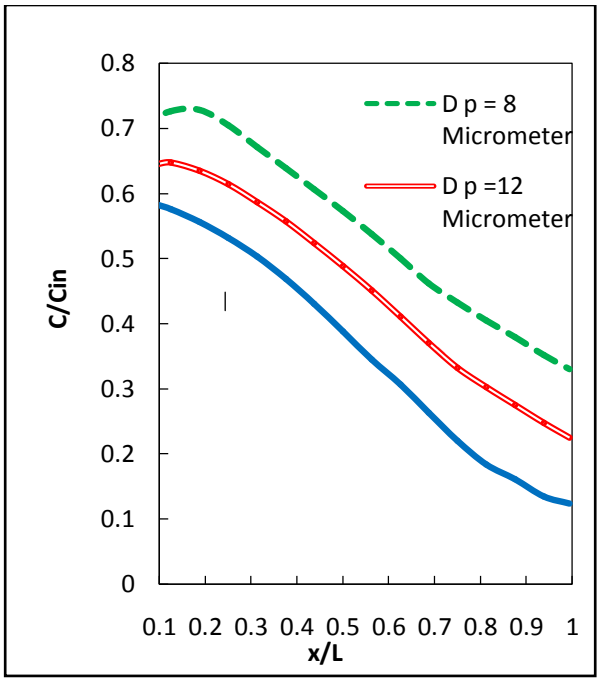

Figure 10: Changes in the mean concentration along the channel

By considering figure 10, the tank efficiency for the three mentioned particle sizes can be determined from the following equation:

$$\eta = \left(1 - \frac{\bar{C}_{out}}{\bar{C}_{in}}\right) \times 100 \qquad (17)$$

The effect of the particle size on the tank efficiency is shown in figure 11. It can be seen that the tank efficiency strongly depends on the particle size and it increases almost linearly with the size of the particles (an increase of 4μm in the particle size leads to an approximately 10% increase in the tank efficiency).

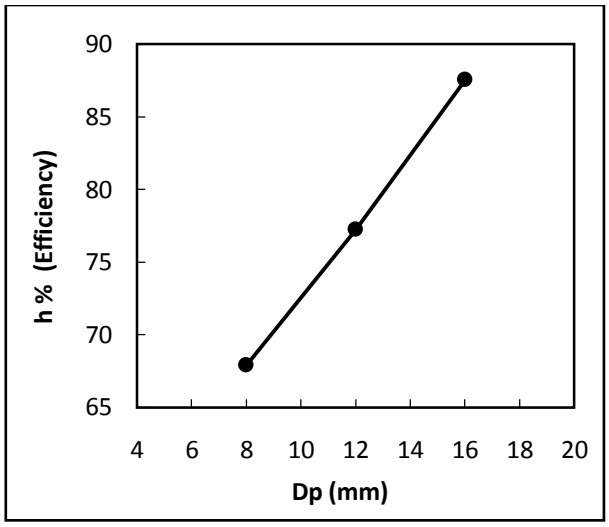

Figure 11: Effect of the particle size on the tank efficiency

5.0 Conclusion

In the present research, the hydrodynamic and efficiency of secondary settling tanks were investigated using a new model. This model considers the effect of the particles on the hydrodynamic, the interaction of particles and the free surface. The obtained velocity and concentration profiles are in good agreement with the experimental results. Comparing the concentration profiles with the experimental data shows the importance of particle size distribution and particle diameter deviation from the mean particle size. Near the inlet, the results of the larger particles show better agreement with the experimental ones.

However, this conformityis reducedat distances far from the inlet. At these distances, the results of the smaller particles show better agreement with the experimental data. Furthermore, we investigated the effect of the particle diameter on the tank performance. The resultsindicate that 4 micrometer increase in the particle sizeresults in an approximately 10 percent increase in the tank performance.

List of symbols

C	Volumetric concentration of particles (-)
D_p	Particle diameter (m)
g'	Reduced gravity acceleration (ms^{-2})

k	Turbulence kinetic energy (m^2s^{-2})
P	Static pressure ($kgm^{-1}s^{-2}$)
$\underset{V}{\rightarrow}$	Velocity vector (ms^{-1})
v_s	Particle settling velocity (ms^{-1})
α	Volume fraction of water
ε	Turbulence energy dissipation (m^2s^{-3})
η	Tank efficiency (-)
μ	Dynamic viscosity ($kgm^{-1}s^{-1}$)
ρ	Density (kgm^{-3})
σ	Surface tension (Nm^{-1})

References

Al-Sammarraee, M., Chan, A., Salim, S., and Mahabaleswar, U., (2009a), Large-eddy simulations of particle sedimentation in a longitudinal sedimentation basin of a water treatment plant. Part I: Particle settling performance: Chemical Engineering Journal, v. 152, p. 307-314.

Asgharzadeh, H., Firoozabadi, B., and Afshin, H., (2011), Experimental investigation of effects of baffle configurations on the performance of a secondary sedimentation tank: Scientia Iranica, v. 18, p. 938-949.

Asgharzadeh, H., Firoozabadi, B., and Afshin, H., (2012), Experimental and Numerical Simulation of the Effect of Particles on Flow Structures in Secondary Sedimentation Tanks: Journal of Applied Fluid Mechanics, v. 5.

El-Bakry, M.Y., Habashy, D., and El-Bakry, M.Y., (2015a), Effect of Particles on Flow Structures in Secondary Sedimentation Tanks Using Neural Network Model: International Journal of Scientific & Engineering Research, v. 6, p. 49-54.

Fan, L., Xu, N., Ke, X., and Shi, H., (2007), Numerical simulation of secondary sedimentation tank for urban wastewater: Journal of the Chinese Institute of Chemical Engineers, v. 38, p. 425-433.

Goula, A.M., Kostoglou, M., Karapantsios, T.D., and Zouboulis, A.I., (2008a), A cfd methodology for the design of sedimentation tanks in potable water treatment: Case study: The influence of a feed flow control baffle: Chemical Engineering Journal, v. 140, p. 110-121.

Imam, E., and Mccorquodale, J.A., (1983), Simulation of flow in rectangular clarifiers: Journal of Environmental Engineering, v. 109, p. 713-730.

Kleine, D., and Reddy, B., (2005), Finite element analysis of flows in secondary settling tanks: International journal for numerical methods in engineering, v. 64, p. 849-876.

Larsen, P., 1977, On the hydraulics of rectangular settling basins: experimental and theoretical studies, Department of Water Resources Engineering, Lund Institute of Technology, University of Lund.

Mccorquodale, J.A., and Zhou, S., (1993), Effects of hydraulic and solids loading on clarifier performance: Journal of hydraulic research, v. 31, p. 461-478.

Stamou, A., and Gkesouli, A., (2015b), Modeling settling tanks for water treatment using computational fluid dynamics: journal of Hydroinformatics, v. 17, p. 745-762.

Tamayol, A., and Firoozabadi, B., (2006), Effects of Turbulent Models and Ba e Position on the Hydrodynamics of Settling Tanks: Scientia Iranica, v. 13, p. 255-260.

Tamayol, A., Firoozabadi, B., and Ahmadi, G., (2008b), Determination of Settling Tanks Performance Using an Eulerian-Lagrangian Method: Journal of Applied Fluid Mechanics, v. 1.

Tamayol, A., Firoozabadi, B., and Ashjari, M., (2009b), Hydrodynamics of secondary settling tanks and increasing their performance using baffles: Journal of Environmental Engineering, v. 136, p. 32-39.

Weller, H., (2002), Derivation, modelling and solution of the conditionally averaged two-phase flow equations: Nabla Ltd, No Technical Report TR/HGW/02.

Yakhot, V., and Orszag, S.A., (1986), Renormalization-group analysis of turbulence: Physical Review Letters, v. 57, p. 1722.